Cell Motility and the Cytoskeleton 61:201–213 (2005)

Symmetry-Breaking in Mammalian Cell Cohort Migration During Tissue Pattern Formation: Role of Random-Walk Persistence

S. Huang,[1] C.P. Brangwynne,[2] K.K. Parker,[2] and D.E. Ingber[1]*

[1]*Vascular Biology Program, Departments of Surgery and Pathology, Children's Hospital and Harvard Medical School, Boston, Massachusetts*
[2]*Division of Engineering and Applied Science, Harvard University, Cambridge, Massachusetts*

Coordinated, cohort cell migration plays an important role in the morphogenesis of tissue patterns in metazoa. However, individual cells intrinsically move in a random walk-like fashion when studied in vitro. Hence, in the absence of an external orchestrating influence or template, the emergence of cohort cell migration must involve a symmetry-breaking event. To study this process, we used a novel experimental system in which multiple capillary endothelial cells exhibit spontaneous and robust cohort migration in the absence of chemical gradients when cultured on micrometer-scale extracellular matrix islands fabricated using microcontact printing. A computational model suggested that directional persistence of random-walk and dynamic mechanical coupling of adjacent cells are the critical control parameters for this symmetry-breaking behavior that is induced in spatially-constrained cell ensembles. The model predicted our finding that fibroblasts, which exhibit a much shorter motility persistence time than endothelial cells, failed to undergo symmetry breaking or produce cohort migration on the matrix islands. These findings suggest that cells have intrinsic motility characteristics that are tuned to match their role in tissue patterning. Our results underscore the importance of studying cell motility in the context of cell populations, and the need to address emergent features in multicellular organisms that arise not only from cell-cell and cell-matrix interactions, but also from properties that are intrinsic to individual cells. Cell Motil. Cytoskeleton 61:201–213, 2005.

Key words: endothelial cell; motility; morphogenesis; development; microfabrication; computational biology

INTRODUCTION

Morphogenesis in multicellular organisms generates structures in tissues characterized by distinct spatial patterns of arrangement of individual cells, and it is often driven by coordinated cell migration. The dynamics of cell motility is often studied in isolated cells plated on planar, open two-dimensional (2D) substrates. In such an environment, a protozoan or metazoan cell will exhibit a migration path that represents a random walk [Dunn and Brown, 1987; Gail and Boone, 1970; Uhlenbeck and Ornstein, 1930]. However, in the formation of patterned arrangements of cells, such as in endothelial and epithe-

S. Huang and C.P. Brangwynne contributed equally to this work.

Contract grant sponsor: NIH; Contract grant number: CA45448; Contract grant sponsor: AFOSR; Contract grant number: F49620-01-1-0564.
*Correspondence to: Donald Ingber, M.D., Ph.D., Karp Family Research Laboratories, Rm 11.127, Vascular Biology Program, Children's Hospital, 300 Longwood Avenue, Boston, MA 02115.
E-mail: donald.ingber@childrens.harvard.edu

Received 11 January 2005; Accepted 13 April 2005

Published online in Wiley InterScience (www. interscience.wiley.com).
DOI: 10.1002/cm.20077

lial structures, cells migrate as a collective and in a coordinated way, so that the tissue appears to flow as a continuous sheet. This type of cohort migration has been visualized in vitro and in vivo [Haga et al., 2004; Nabeshima et al., 1999; Schock and Perrimon, 2002], but the dynamic principles underlying genesis of these coupled movements is difficult to study.

How is the isotropy of random walk motility of individual cells harnessed and converted into a directional cohort migration? One traditional explanation is the presence of external factors, such as chemotactic or haptotactic cues that create a gradient and direct all the cells to move in one direction along the gradient. However, these external cues do not actually explain pattern formation at its very core, for one then would have to explain how the asymmetry of the external gradient itself is established. In contrast, from a strictly ontological point of view, pattern formation is a spontaneous, self-organizing process that occurs without external cues or a template. Hence, pattern formation must involve a "symmetric breaking event" [Beloussov, 1993; Kirschner et al., 2000] arising from its internal dynamics, which in the case of coordinated cohort migration, overcomes the intrinsic symmetry of the random walk (i.e., symmetrical probability to move in any direction). Such spontaneous breaks of symmetry have been modeled in the past for the spatiotemporal distribution of diffusible chemical morphogens in diffusion-reaction systems, and this paradigm also has been proposed to apply to migrating cells [Murray, 1993; Nijhout, 1997]. Cells exhibit random-walk behavior when they migrate on planar substrates, and thus potentially could be modeled like diffusing molecules. However, the reality is that most cells move within tightly packed cell layers in living tissues, and create spatial patterns (e.g., branching capillary networks) with characteristic lengths on the micrometer scale within a microenvironment that is saturated with multiple chemical growth factors [Huang and Ingber, 1999]. In vitro studies have shown that cell motility can be spatially constrained to thin paths by selective adhesion to insoluble extracellular matrix (ECM) proteins [Dike et al., 1999] and to neighboring cells [Gumbiner, 1996], which govern directionality, even if motility is globally stimulated by soluble factors. Cell migration is also strongly influenced by the surface features of the microenvironment, as recently documented with artificial substrata [Curtis and Wilkinson, 1998; Matsuda and Sugawara, 1996; Parker et al., 2002]. Moreover, cells are complex systems that can influence each other's migratory behavior.

We recently described a novel model system in which symmetry-breaking events can be reproducibly induced in capillary endothelial (CE) cells that are migrating on micrometer-scale ECM islands created with microcontact printing technology, which physically constrain the area over which cells can move [Brangwynne et al., 2000; Chen et al., 1997]. To examine how spatial constraints can impact symmetry-breaking in migrating cells, we cultured multiple CE cells on single islands coated with the ECM protein fibronectin that were between 30 and 50 μm in width. These culture conditions suppress random-walk behavior, and promote spontaneous symmetry-breaking, as indicated by coordinated migration of adjacent CE cells in the absence of a gradient of soluble or immobilized chemotactic factors. Here we analyze this response and use a computer model to establish that the symmetry-breaking event and ensuing coordinated locomotion critically depend on the value of two control parameters: directional persistence of the random walk and dynamic mechanical coupling.

MATERIALS AND METHODS

Experimental System

Micropatterned substrates containing round (50 μ diameter) or square (20–50 μm in width) fibronectin islands were created on glass slides by microcontact printing [Chen et al., 2000] and coated with a high-density (50 μg/mL) of fibronectin, as described [Chen et al., 1997]. Bovine CE cells and mouse NIH 3T3 fibroblasts were cultured, as previously described [Parker et al., 2002], trypsinized and plated at 6×10^3 cells/cm^2 on the micropatterned substrates so that individual islands were seeded with 2 or more cells. Studies on the microscope were carried out in experimental bicarbonate-free minimum essential medium (MEM) containing Hank's balanced salts lacking phenol red and bicarbonate (Sigma Chemical Co., St. Louis, MO), MEM amino acids (Sigma), MEM vitamins (Sigma), 2 mM L-glutamine, 1 mM sodium pyruvate, 20 mM N-2-hydroxyethylpiperazine-N′-2-ethanesulfonic acid, D-glucose (1 g/L), hydrocortisone (1 μg/ml), and 1% bovine serum albumin (BSA; Intergen Co., Purchase, NY; Cohn fraction V, pH 7.0). This medium was supplemented with 20 μg/mL high-density lipoprotein (Bionetics Research, Rockville, MD) and 5 μg/mL transferrin (Collaborative Research, Lexington, MA) for studies with CE cells. Studies with fibroblasts used the same medium with high glucose (5 g/L). Migratory behavior was stimulated by addition of human PDGF-BB (5 ng/mL) for NIH 3T3s, and basic FGF (5 ng/mL) or 10% calf serum in CE cells. For some studies, 10% FBS was used with similar results. Migratory behavior was visualized with a Hamamatsu CCD camera on a Nikon Diaphot 300 inverted microscope equipped with phase contrast optics and epifluorescence illumination. Temperature was controlled by a stage mount (Micro Video Instruments, Avon, MA) equipped

with a temperature regulator (Omega Technologies Co., Stamford, CT).

The velocity of moving cell ensembles was calculated by tracking the rotation of a line segment connecting the geometric center of the nuclei whose coordinated movement was monitored during time-lapse video microscopy. Time-lapse microscopy experiments varied from 4 to >24 h in duration. In order to determine if cohort migration was limited to mother/daughter-cell pairs following cell division of a cell on an island, cells were marked with a fluorescent marker (CellTracker, Molecular Probes, Eugene, OR), mixed at equal ratio with unmarked cells, and plated on micropatterned FN islands. Immunohistochemical staining of tubulin and DNA (nuclei) in paraformaldehyde-fixed cells was accomplished using fluoresceinated rabbit anti-tubulin antibody, and DAPI (both from Sigma) respectively. Immunofluorescence microscopy was carried out using the epifluorescence optics of the Nikon Diaphot microscope.

Mathematical Model

Spatially ordered migration of two cells on a single ECM island was modeled as a system consisting of two rigid point objects (cells *a* and *b*) migrating in a random-walk on a circular track with angular position ϕ_i(t), for cell $i = a$, or *b*. Cell motility in discrete time was driven by a stochastic cellular automaton model containing two cells. After each time step, Δt, the cells move by a constant minimal step of Δd on the circle (or stand still), representing a "microscopic" velocity, defined by $\omega_i \in \{-1,0,1\}$ for {clockwise motion, unpolarized stasis, counterclockwise motion}. The "macroscopic" displacement of the cells results from the addition of the minimal steps, $\Sigma_n(\Delta t_n\ \omega_n)$ over discrete time. The value for the directional velocity ω_i was updated according to a rule that biased the probabilities *P* of the new velocity values as a function of previous velocity of each cell and angular distance between the cells:

$$\omega_i(t+1) = f_{p,c}[\omega_i(t), \omega_j(t), \delta] \tag{1}$$

where δ is the angular distance $|\phi_i - \phi_j|$ between the two cells. The parameters for coupling, *c*, and persistence, *p*, introduce a linear bias to the probabilistic updating function $f_{p,c}$. The bias was determined in a Monte Carlo method with a geometric probability space that implemented the following assumptions:

1. Linear repulsion potential *R* as δ approaches 0, the probability for the event that both cells move towards each other goes linearly to zero, while at $\delta = \pi$ there is no bias for the value of ω, i.e., $P[\omega(t) = 1] = P[\omega(t) = -1] = P[\omega(t) = 0]$. *R* was kept constant through all simulations.
2. The persistence bias *p* increases the probability $P[\omega_i(t+1) = \omega_i(t)]$ that a cell will keep moving in the same direction, thus reducing the sensitivity to random fluctuation. For the parameter value $p = 1$ there is "total persistence," $P[\omega_i(t+1) = \omega_i(t)] = 1$, while for $p = 0$, $P[\omega_i(t+1)]$ is unbiased by $\omega_i(t)$.
3. The dynamic coupling bias *c* increases the probability $P[\omega_i(t+1)] = \omega_j(t)]$ that a cell follows the previous direction of the other cell, as justified above. Thus for $c = 1$, there is total coupling, $P[\omega_i(t+1)] = \omega_j(t)] = 1$ while with $c = 0$, cells move absolutely independent from each other.

Implementation of the updating function $f_{p,c}$ in (1). The new velocity value $\omega(t+1)$ is generated in a probabilistic fashion as follows:

$$\omega_i(t+1) = \begin{cases} -1 & 0 \le S < s_1 \\ 0 & s_1 \le S < s_2 \\ 1 & s_2 \le S < 1 \end{cases} \tag{2}$$

where *S* is a uniformly distributed random number [0,1]. At each time step, *S* is drawn and compared to the boundaries s_1 and s_2 in eq. (2), which are determined by the arguments of $f_{p,c}$ in (1) in the following way: First, the relative angular position δ introduces a *basic bias* that captures the repulsion (steric hindrance due to finite cell dimensions) as described above: $s_1 = R_1(\delta)$ and $s_2 = R_2(\delta)$. The functions *R* are piecewise linear functions of δ or $\varepsilon = 2\pi - \delta$, respectively, [depending on constellation σ = sign $(\phi_a - \phi_b)$]. *R* are defined such that at $\delta = \pi$ (when cells are at opposite sides of the circle), $s_1 = 1/3$ and $s_2 = 2/3$, corresponding to equal probabilities for all three values of $\omega_a(t+1)$ (2). In contrast (for the example of cell *a* in the constellation σ = positive) at $\delta = 0$, $s_1 = 0$ and $s_2 = 1/2$ so that cell *a* has either to move with $\omega_a(t+1) = 1$, i.e., increasing δ, or to rest, $\omega_a(t+1) = 0$, with equal probability 1/2. On top of the bias from the repulsion *R*, the boundaries *s* are biased by *p* and *c*

$$s_1 = R_1(\delta_t) + f_p^a p + f_c^a c$$

and (3)

$$s_2 = R_2(\delta_t) + f_p^a p + f_c^a c$$

The persistence *p* is implemented by the rule function f_p for cells *a* or *b*, respectively, which introduces a conditional shift of the boundaries s_i in eq. (2) so as to linearly increase the probability for $[\omega(t+1)=\omega(t)]$ for a

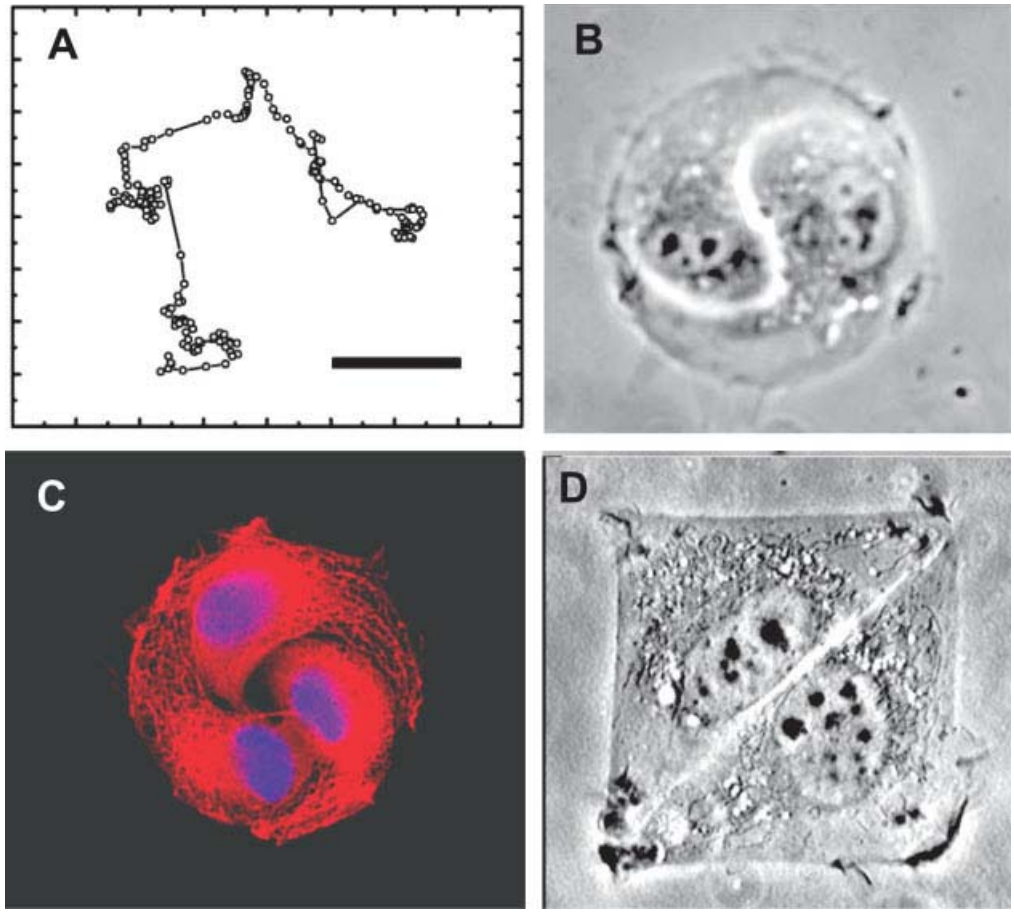

Fig. 1. Geometric constraints on random walk. **A:** Example trajectory of an adherent mammalian cell showing the intrinsic persistent random walk behavior in the absence of any external cues. Time interval between positions (*circles*) is 1 min. Scale bar = 10 μm. **B:** Two BCE cells on a 50-μm diameter circle showing YY pattern. **C:** Immunofluorescence picture of three bovine CE cells on a 50-μm diameter circle showing stable YY pattern observed in groups of more than two cells, immunostained for tubulin (*red*). Nuclei (*blue*) visualized by DAPI stain. D: Two NIH 3T3 cells on a 50- × 50-μm square whose cell–cell interface does not display the characteristic sigmoidal shape but typically forms along the diagonal of the square.

given cell by a magnitude determined by the cofactor p, according to (3). For cell a, the rule function is as follows:

$$f_p^a = \begin{cases} 1 & \omega_a(t) = -1 \\ 0 & \omega_a(t) = 0 \\ -1 & \omega_a(t) = 1 \end{cases} \quad (4)$$

In contrast, for the coupling, the rule function f_c introduces a bias in an analogous way such that the probability is increased for $\omega_a(t+1) = \omega_b(t)$. Hence, the rules for cell a contain a cross-reference between the two cells:

$$f_c^a = \begin{cases} 1 & \omega_b(t) = -1 \\ 0 & \omega_b(t) = 0 \\ -1 & \omega_b(t) = 1 \end{cases} \quad (5)$$

RESULTS

Experimental Symmetry-Breaking and Coordinated Cell Migration

In the absence of directional cues, cultured cells that are free to move in two dimensions exhibit a random-walk with a characteristic trail, as shown in Figure 1A [Dunn and Brown, 1987; Gail and Boone, 1970; Uhlenbeck and Ornstein, 1930]. In living tissues, this intrinsic cell movement is constrained by neighboring cells and surrounding ECM in the local microenvironment. To mimic these spatial constraints that cells encounter within tissues in an experimentally controlled way, we cultured CE cells on fibronectin-coated islands surrounded by non-adhesive (fibronectin-free) regions, so that cell attachment and migration were confined to the adhesive areas that were polygonal (square or circular) in form. These geometrically-defined planar substrata were created using microcontact printing, which

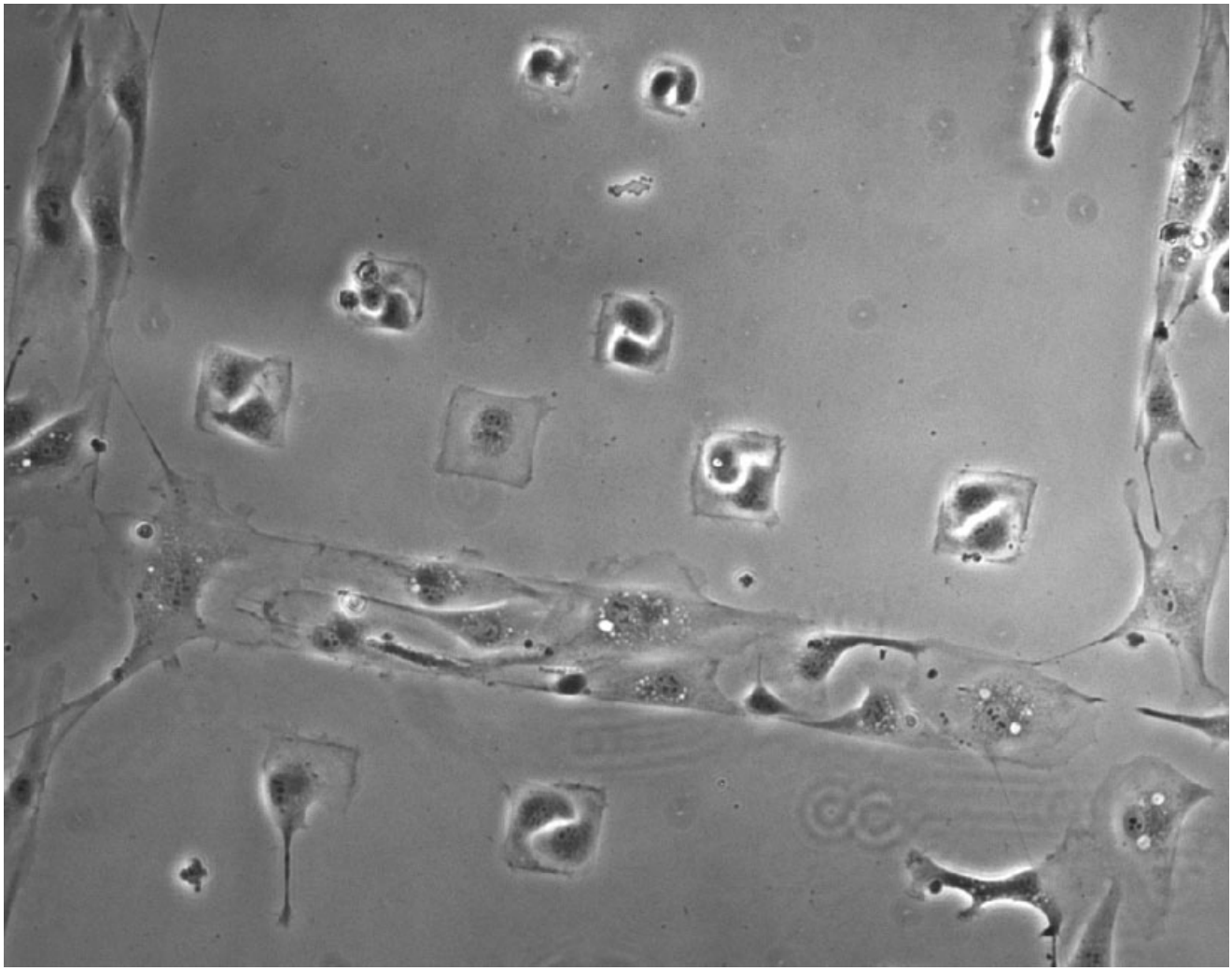

Fig. 2. Robustness of YY patterns. Phase contrast image of a surface micropatterned with an array of squares of different sizes and plated with BCE cells. Of the 8 pairs of cells that occupy 30- × 30-, 40- × 40-, and 50- × 50-μm squares, all of them show the characteristic YY shape. Note that cells in the long rectangular border regions show no such patterning. Single cells on squares also do not exhibit YY patterning.

allows us to fabricate ECM islands of any desired shape [Brangwynne et al., 2000; Brock et al., 2003]. When plated on these substrata, single CE cells attach and spread to fill each fibronectin island when they are 50 μ in diameter or smaller; on larger islands (e.g., 100 μm), CE cells adhered and migrated primarily along the edge of the island but in a random direction. When two cells adhered to the same micrometer-sized circular (Fig. 1B) or square (Fig. 2) fibronectin islands, the cells spread until they reached the outer edge and fully contacted one another. This resulted in complete coverage of the entire island by two cells with a continuous, S-shaped cell–cell contact line stretching across the island, giving the island an appearance that is reminiscent of a Yin-Yang (YY) symbol (Fig. 1B). As previously shown, these cells exhibit a coordinated migration in that both CE cells rotate around the geometric center of the two-cell system in the same direction [Brangwynne et al., 2000], thus breaking the symmetry of random walk to engage in cohort locomotion. The S-shaped cell–cell interface is formed because each CE cell is led by a lamellipodium that wraps around the trailing edge of the adjacent cell. When a single adhesive island was occupied by more than two CE cells, all the cells rotated in a coordinated manner in the same direction around a central vortex, giving rise to a "multi-cell YY" of three to six cells (Fig. 1C). [A time-lapse movie of rotating CE cells in a YY configuration can be viewed at: http://www.childrens-hospital.org/research/ingber/YYmovie.qt]. Furthermore, when fluorescently-labeled cells were mixed 1:1 with

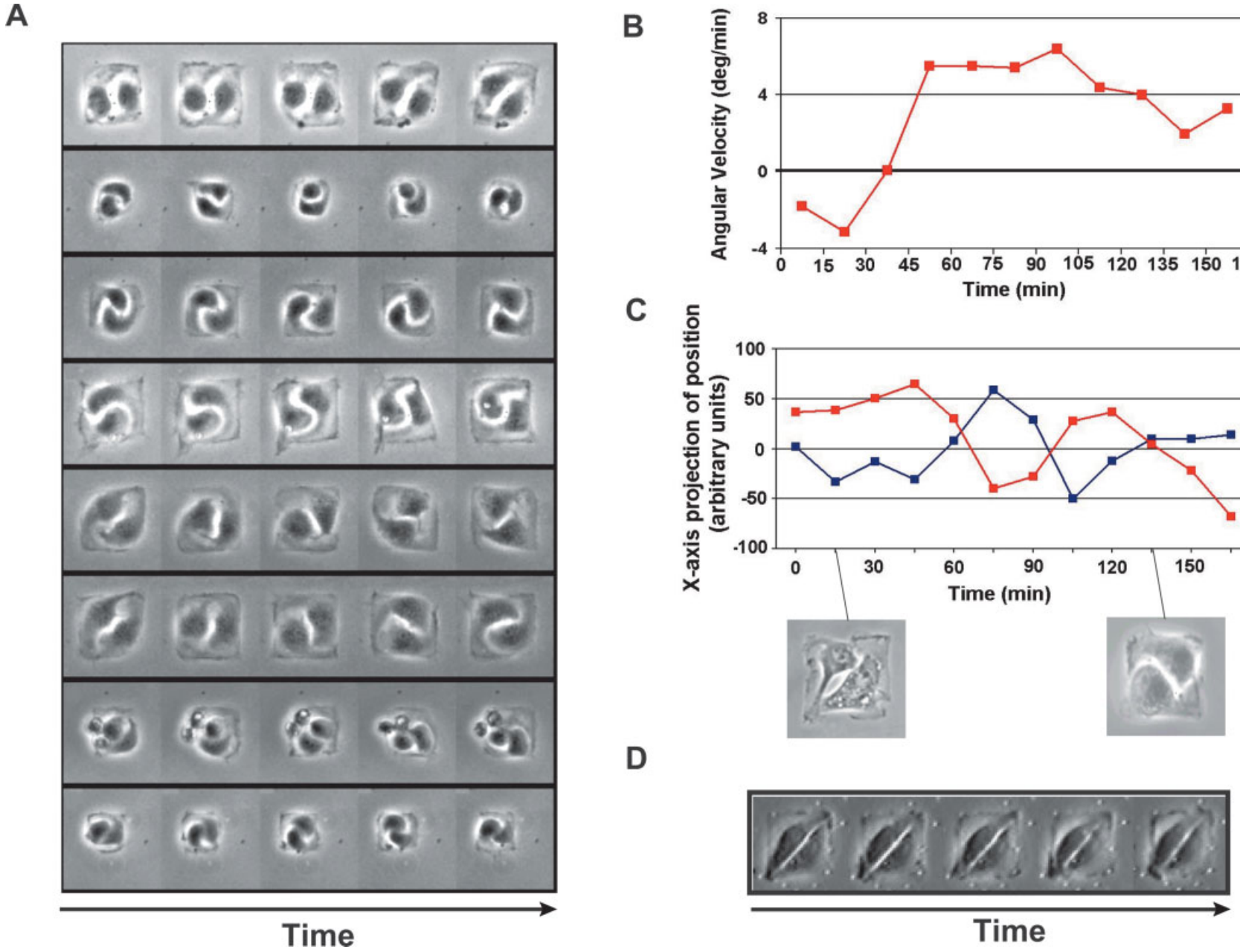
A
Time
B
Angular Velocity (deg/min)
8
4
0
-4
0 15 30 45 60 75 90 105 120 135 150 175
Time (min)
C
X-axis projection of position (arbitrary units)
100
50
0
-50
-100
0 30 60 90 120 150
Time (min)
D
Time

Figure 3.

unlabeled cells and plated on the same islands, YY patterns were often found to contain mixtures of labeled and unlabeled cells, thus confirming that cell division was not required for this behavior.

When viewed at a lower magnification, we found that coordinated YY rotation arose on >95% of the adhesive island occupied by two or more CE cells, demonstrating the robustness of both the symmetry-breaking event and the coordinated migration (Fig. 2). In contrast, on neighboring fibronectin regions that were geometrically unconstrained (e.g., stripe-like borders between patterned regions in Fig. 2), the CE cells continued to move in random walks as individual entities. The YY rotation was insensitive to variations of the geometry or size of the island since similar results were obtained with cells on circular and square islands ranging from 30 to 50 μm in diameter. Thus, the spontaneous formation of YY patterns and the coordinated cohort migration that drives this process, appear to be intrinsically robust for the CE cells. Interestingly, in contrast to CE cells, fibroblasts did not rotate or exhibit YY behavior when cultured on the same microfabricated fibronectin islands, although they migrate rapidly when plated on the unconstrained fibronectin substrates [Sells et al., 1999; Ware et al., 1998]. Instead of exhibiting an S-shape, cell–cell interface like the CE cells, fibroblasts formed a straight cell–cell boundary that stretched diagonally between opposite corners of the square islands (Fig. 1D).

We next quantitated the rotational movements associated with the YY patterns by analyzing movie frames from CE cell pairs cultured on 8 different fibronectin islands (Fig. 3A). Tracking of the movements of individual CE cells revealed that after a brief period of initial "undecidedness" marked by negative and then positive angular velocity (representative velocity graph in Fig. 3B), both cells began to rotate in a coordinated manner in either a clockwise or counterclockwise manner with equal probability. This transient dynamic instability was observed only during the short time period when cells had not yet fully covered the surface of the entire fibronectin island (Fig. 3C). After symmetry-breaking, cells migrated in a coordinated manner at a constant average velocity of 3–6°/minute; these rotational movements were maintained over the entire 24-h period we studied. Tracking the position of pairs of cells on the same island revealed two sinusoidal curves with a phase shift of 180°, consistent with the coordinated YY rotation (Fig. 3C).

The lack of coordinated migration in fibroblasts under these spatially constrained conditions (Fig. 3D) was not expected because fibroblasts display random walk motility on standard, fibronectin-coated culture substrates in the presence of serum and soluble motility factors [Sells et al., 1999; Ware et al., 1998]. However, fibroblasts differ from endothelial cells in that their unconstrained random-walk behavior is characterized by a much lower persistence time. This refers to the average duration of locomotion in one direction before a random change of direction, and it is an order of magnitude shorter in fibroblasts than in endothelial cells [Stokes et al., 1991; Ware et al., 1998].

Taken together, these experimental observations suggest a set of minimal requirements for the symmetry-breaking that might overcome the intrinsic random walk behavior: (1) spatial constraint of cell migration; (2) a long persistence time of the random walk; and (3) physical contact ("coupling") between cells. Under these conditions, the intrinsic randomness of individual cell motility may be subjugated to the robust, coordinated cohort migration that is necessary for generation of tissue-level YY patterns.

Model Description

To examine whether these three minimal requirements are sufficient to generate the coordinated and directed movement responsible for generation of the YY-pattern, we developed a minimal model based on a discrete, stochastic one-dimensional cellular automaton (see Fig. 4A, Material and Methods). This idealized model of two cells captures the essential experimentally observed features described above:

1. *Spatial constraint of migration:* Two cells move in a random walk along a circular track as rigid objects. This spatial constraint not only recapitulates the reduced degrees of freedom of cell migration in the crowded tissue environment, but was also motivated by our observations and those of others [Clark et al., 1991; Matsuda and Sugawara 1996], which indicate that cells on micropatterned surfaces preferentially adhere

Fig. 3. Quantitative characterization of Yin-Yang rotation. **A:** Time series (phase contrast) images of each of the 8 pairs of cells shown in Figure 2. Each row shows a different pair of cells at 5 different time points separated by 15.5 min. Stable migration of each pair in either the clockwise or counterclockwise direction is evident. **B:** Angular velocity of an example trajectory of a pair of YY cells showing an initial unsteady phase of about 40 min followed by stable rotation in the counterclockwise direction at an average angular velocity of about 4°/min. **C:** Time evolution of the projection of the x-axis coordinate of the nuclei of each cell in the same YY pair analyzed in B. The initial unsteady phase is followed by symmetry-breaking into a stable oscillatory YY migration behavior. **Insets:** Movie frames of cells in the phase before and after symmetry break. **D:** Time series images of a typical pair of NIH 3T3 cells on a 50-μm square. Images are separated by 15.5 min. The cells show no net migration.

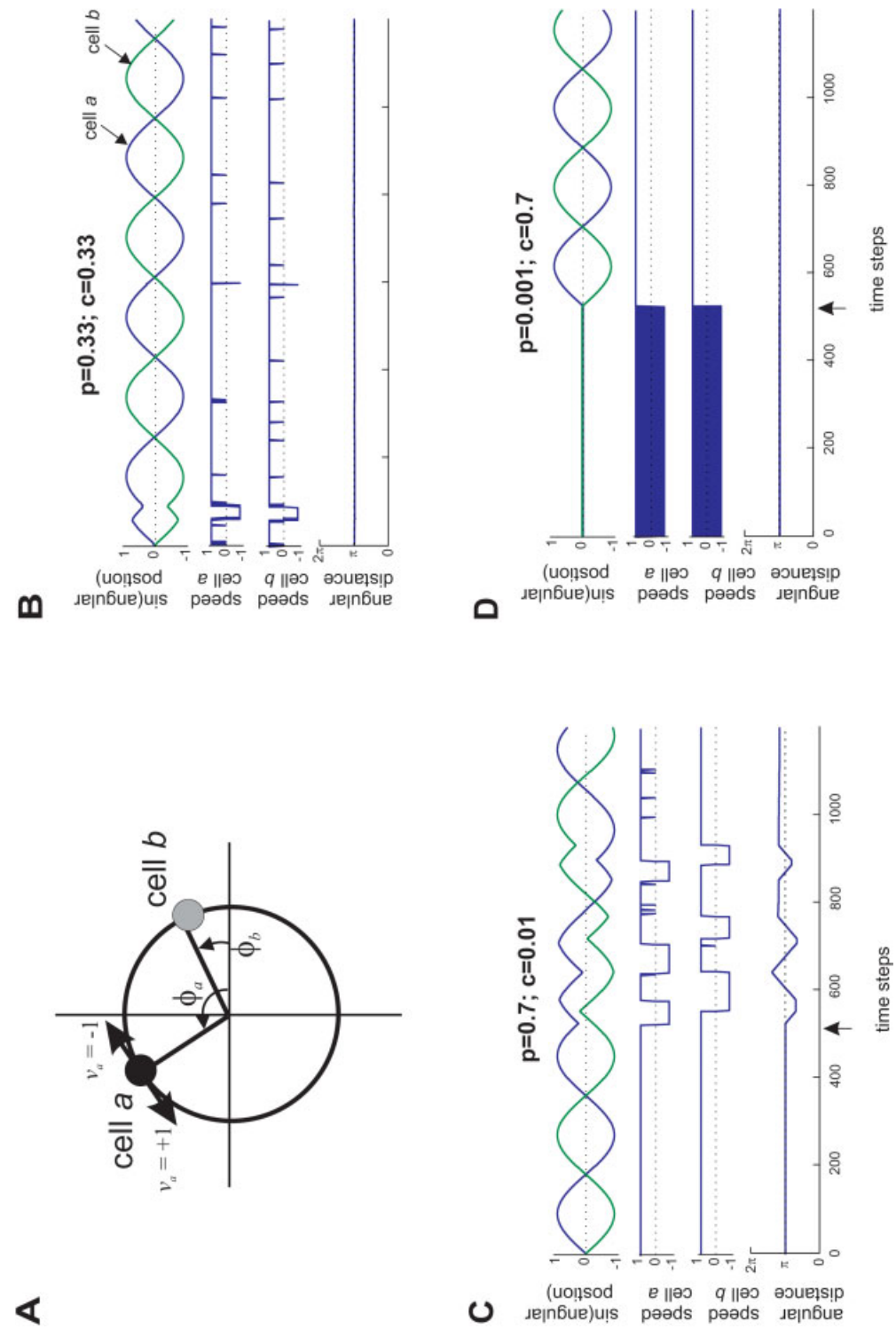

Fig. 4. A simple model for the YY-rotation. **A:** One-dimensional probabilistic cellular automaton model for cohort migration (see text for details). **B–D:** Results of computer simulations of the two-cell system for different values of p and c. Angular position, the speed of each cell, and the angular distance between the two cells are depicted versus time (simulations were run for 1,200 time steps). *Arrows* indicate external perturbation that pushes cell a in the opposite direction, overriding the update rules. **B:** Stable, near-perfect YY behavior. **C:** Perfect YY behavior prior to the perturbation, followed by a transient exit from the YY mode. **D:** Random motility prior to the perturbation that induces YY behavior.

and move along linear adhesive substrates, such as aligned ECM fibrils, linear islands, or the outer edge of the polygonal adhesive islands. This reduces the dimensionality of the stochastic locomotion from 2D to one dimension (1D), and allows for the use of a 1D random walk.

2. *Persistence:* A characteristic of random walks as representations of physical displacements is the influence of the persistence of directionality on net displacement, i.e., the resistance of the velocity vector to random fluctuations [Dunn and Brown, 1987]. Persistence p can be expressed as the average time period in which the cell moves without changing direction and can be measured from the short-time ballistic regime of the mean squared displacement $<x^2(t)>$ of randomly walking cells [Dunn, 1983]. Persistence time has been measured in the past for several migratory cells [Sells et al., 1999; Stokes et al., 1991; Ware et al., 1998]. In the model, the degree of persistence is represented by the parameter p ($0 < p < 1$).
3. *Coupling:* The direction of cell migration can be affected by the motion of neighboring cells through direct physical contact, as we have observed between CE cells. For instance, tapping on the "back" of a cell (e.g., with a pipette) can induce "forward" motion [Verkhovsky et al., 1999]. Alternatively, under conditions of spatial constraint, the tendency of cells to spread into areas of the fibronectin substrate that become exposed when the adjacent cell moves away from those sites also may contribute to motility coupling. Irrespective of the detailed mechanism responsible for correlative migration, we captured this tendency of a cell to move in the same direction as its adjacent neighbor with the parameter for dynamic (mechanical) coupling c ($0 < c < 1$) (see Material and Methods for details).

Simulation Results

We then asked whether, given the obvious geometrical constraints, the two core properties of our minimal two-cell system—directional persistence of random motility(p) and dynamic mechanical coupling (c)—are sufficient to convert the intrinsically stochastic motion of cells into coordinated, directional migratory behavior. Figure 4 shows representative examples of the simulation of the model for three different pairs of p and c parameter values. For intermediate values ($p = 0.33$; $c = 0.33$), after a brief initial phase of uncorrelated movement due to the intrinsic stochastic motility of the individual cells, the motion of both cells abruptly became locked in a parallel, net clockwise or counterclockwise displacement on the circular track (Fig. 4B). This initial instability and ensuing symmetry-breaking was strikingly similar to that observed in experiments that led to YY behavior of CE cells (Fig. 3C). This state of coordinated YY-like rotational motility was stable to external perturbations, which in the model was implemented by externally forcing one cell to move into a single direction for 10 time steps; this perturbation did not result in visible transients. In contrast, coordinated cell rotation did not occur at very low values of both persistence and coupling ($p \cong c \cong 0$). Instead, random oscillatory motion was observed that did not produce any net displacement of the cells (not shown).

At higher values of either p or c, correlated cell motion (high "Yin-Yang-ness" as defined below) was still possible; however, it was not stable and could be transiently disturbed. For values of high persistence ($p = 0.7$) but low coupling ($c = 0.01$), the same perturbation triggered a transition from correlated rotation to transient irregular motion (Fig. 4C) which could spontaneously fall back to the coupled migration mode. Conversely, for low persistence but high coupling (e.g., $p = 0.001$ and $c = 0.7$), the two cells moved randomly and independently, and failed to exhibit a net displacement (Fig. 4D). A transient perturbation (as used above), however, could push the system into the smooth correlated rotation mode, which for these parameter values again was unstable to further perturbations. Together, these simulations indicate that in a confined space, the cell's inherent random locomotion will be unstable and undergo symmetry-breaking giving rise to the coordinated cohort migration of YY behavior if individual cells exhibit some minimal degree of both persistence and dynamic physical coupling.

To quantify this, we determined the relative robustness of YY pattern-forming behavior for the entire p/c parameter space. For these simulations, an order parameter, Y ("Yin-Yang-ness"), was defined as the fraction of time in which the cells moved in parallel and exhibited net rotation during the observation period of T time steps, Δt:

$$Y = \sum_{t=t_0}^{t_0+T} \mu_t / T$$

where $\mu_t = 1$ if $|<\omega_a(t)> - <\omega_b(t)>| < \varepsilon$ *and* if $|<\omega_i(t)> - 1| < \varepsilon$; else $\mu_t = 0$. The expression $<\omega_i(t)>$ denotes the time average of the velocity value for cell a and/or b over a period $\tau \ll T$ around t. As expected from individual simulations, a gradient along the diagonal from (low p ,low c) to (high p, high c) regions is immediately visible. The cells exhibited spontaneous, stable, and smooth *YY* rotation behavior already at parameter values

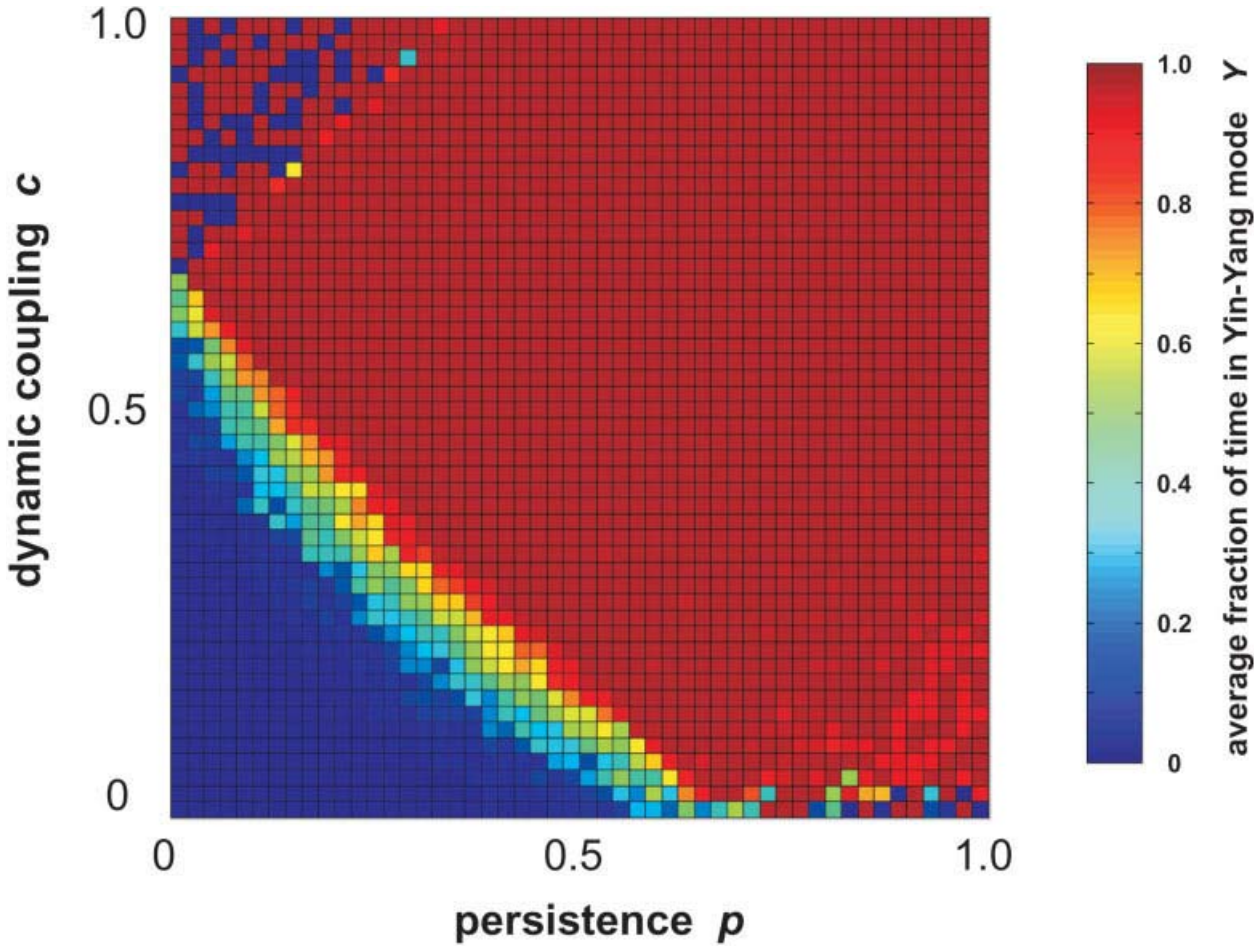

Fig. 5. The *p*,*c*-parameter space and expression of YY behavior. Simulations were run for parameter pairs p and c for values from 0 to 1 each, with increments of 0.02. For each pair of p, c values, pseudocolors, as indicated in the color bar, represent the value of the order parameter Y (average fraction of time in YY mode over a period of $T = 1{,}200$ time steps).

$p > 0.4$ and $c > 0.4$. Thus, the regime for stable concerted rotation is relatively large. However, the different responses in the corners of the parameter space where p is low and c is high (and vice versa) suggest that there is a qualitative difference between the role of these two properties in determining correlated rotation. At regions of high coupling but low persistence (top left corner of graph in Fig. 5), cells either exhibit perfect rotational coupling of cell migration (maximum Y value) or move in a totally uncorrelated manner ($Y = 0$) as was shown in Figure 4D. Repeated simulations indicate that in this regime, cells randomly chose either one of these modes, but none exhibit the intermediate *Y values* (Fig. 4D). In contrast to this all-or-none regime, in the corner of the parameter space with high persistence and low coupling, the Y values did not converge over time and cells exhibited randomly distributed intermediate average values of Y, indicating partial coupling of cell rotation as seen in the second part of the simulation in Figure 4C.

Fibroblast cells, which do not generate YY patterns (Figs. 1D, 3D), have a persistence time of $p = 20$–30 min, an order of magnitude shorter than that exhibited by CE cells ($p = 3$–6 h) that consistently exhibit this simplified form of tissue pattern formation [Brangwynne et al., 2000; Stokes et al., 1991; Ware et al., 1998]. This observation is consistent with our qualitative model's prediction that systems with low values of directional persistence will not produce persistent coordinated migration unless the level of cell–cell coupling is extremely high. Given that fibroblasts commonly move individually, and not as elements of cellular sheets (e.g., as in epithelium or endothelium), they likely have low values of coupling c. In this case, the model predicts that frequent turns of direction due to the random motility of each fibroblast cell will overcome a weak dynamic coupling and prevent the symmetry-breaking transition; thus, YY pattern formation would not occur, as we observed experimentally.

DISCUSSION

Understanding how specific spatial patterns develop in growing tissues remains one of the most fundamental questions in cell and developmental biology. In all systems, symmetry-breaking driven by the internal dynamics is at the heart of spontaneous pattern formation [Beloussov, 1993; Kirschner et al., 2000]. Here we studied the simplest possible model of mammalian tissue pattern formation, generation of a YY-like pattern within a tissue composed of as few as 2 cells. The robust, coordinated cell rotation that drives YY pattern formation arises spontaneously by breaking the symmetry of the intrinsically random (hence, symmetrical) motility of the component cells. Experimental observation and a generic computer model suggest that there are 3 conditions that together are necessary and sufficient for this symmetry-break of random motility. First, the space available for cell migration must be physically constrained on the micrometer scale. Second, for cells to generate the YY pattern, their intrinsic random walk behavior must exhibit a long persistence time. And, finally, there must be dynamical coupling of motility between cells, potentially through mechanical interactions between the contacting cells, or through dynamic adhesive interactions with exposed regions of the ECM substrate. These studies also demonstrate that this microfabricated culture system provides a minimal, geometrically defined pattern-forming tissue module that is experimentally accessible. This experimental system may, therefore, be useful for the study of the core dynamic events involved in the self-organized, collective cell motility that underlies the morphogenesis of many tissue patterns. It is important to note that our computer simulation is an idealized, abstract, and generic model aimed at understanding the *minimal* constraints that can give rise to the observed spontaneous ensemble behavior. Thus, our approach differs from those modeling approaches more familiar to engineers in which as many specific mechanistic details as possible are incorporated to construct a model that faithfully mimics the function of one specific embodiment of a system *in silico*.

The spontaneous coordination of cell migration studied here represents a novel ordering principle for cell rearrangement because the only mechanisms known thus far that impose regularity onto intrinsically random cell locomotion behavior in vivo are the external influences of soluble chemotactic factors (i.e., motility factors) or insoluble haptotatic factors (e.g., ECM components). Chemotaxis or haptotaxis may play a role in patterns at a larger size scale, where the characteristic length of pattern features (such as coat stripes, spots) are orders of magnitudes larger than their underlying component parts (diffusing morphogens, pigments). These patterns can be modeled as diffusion-reaction systems with partial differential equations or using cellular automata [Ermentrout and Edelstein-Keshet, 1993; Murray, 1993; Nijhout, 1997; Palsson and Cox, 1996; Stocker, 1999; Turing, 1952]. In contrast, such mechanisms are unlikely to be entirely responsible for structures that form patterns through cell rearrangements on the scale of a few cell diameters within a microenvironment that is saturated with soluble chemical stimuli, as is observed during formation of epithelial buds and capillary branches during tissue morphogenesis [Huang and Ingber, 1999; Moore et al., 2002]. Symmetry-breaking events in cell biology have been described previously, but at a smaller size scale within the cytoskeleton of a single cell [Kirschner et al., 2000; van Oudenaarden and Theriot, 1999].

The two-cell system on a fibronectin island is, of course, an experimental idealization. Confined areas for cohort migration in vivo, such as during embryonic development, often contain moving sheets of tens to hundreds of cells. Once cells cultured on standard (unconstrained) 2D plastic substrate increase their density, they also impose geometric constraints and enforce mechanical cell–cell coupling between neighboring cells. In fact, the "wave and swirl" patterns of cell arrangement observed in confluent CE cell monolayers and sheets of cultured MDCK cells may result from collective movements due to local mechanical coupling [Folkman and Haudenschild, 1980; Haga et al., 2004] similar to those described in our simplified model system.

Coherent migration of large populations of cells is not limited to metazoan cells. Microoorganisms have been shown to exhibit cohort migration [Ben-Jacob et al., 1998], of which the most prosaic example is the case of slime mold (*D. discoideum*), where wave-like cohort migration precedes the transition from a single cell growth form to the aggregation of a multicellular mold. In this case, the predominant factor that enables cohort migration is chemical coupling mediated by pulse-secreted and diffusing cAMP [Rietdorf et al., 1996]. However, important aspects of this cohort migration have been shown to be independent of cAMP signaling and may reflect intrinsic migration behavior and local cell–cell coupling [Rappel et al., 1999]. Such multicell pattern formation has been modeled using a variety of discrete automata approaches [Glazier and Graner, 1993; Levine et al., 2001; Rappel et al., 1999]. These models share the common feature that each cell only interacts with its immediate neighbors. One of the simplest models of this type involves self-propelled random-walkers, which are biased to move in the average direction that their neighbors are moving [Vicsek et al., 1995]. This represents a kinetic analogue to the well-known magnetic spin lattice models and has been shown to undergo a similar symmetry-breaking phase transition where local interactions propagate order across the sys-

tem and all the particles begin moving in the same direction. Similar kinds of behavioral phase transitions have been observed in organismic biology models of foraging ants [Beekman et al., 2001]. Our theoretical approach complements and extends these ideas and underscores the importance of both local constraints and the persistent directionality of cells in determining the structure of the emergent pattern. Indeed, preliminary extension of our two-cell, 1D-model to a 2D-mass of many cells suggests that the details of the resultant cohort migration depend sensitively on directional persistence (Brangwynne, unpublished observations).

Given the significance of persistence time for symmetry-breaking and cohort migration, the wide range of persistence times among various cell types may reflect their distinct roles in tissue dynamics. Fibroblasts, which have low persistence time, do not form distinct tissue architectures, but rather act to fill the connective tissue space between the epithelial, endothelial, and nerve structures. In fact, fibroblasts only form minimal cell–cell contacts and, thus, they may also exhibit low values of our coupling parameter c. Consistent with the predictions of our mathematical model, their migratory characteristics (low persistence time and little coupling) do not promote cohort migration. Interestingly, directional persistence in leukocytes is also more than tenfold lower than that of CE cells [Farrell et al., 1990; Stokes et al., 1991; Ware et al., 1998; Zigmond et al., 1985]. This is noteworthy because leukocytes act physiologically as individual cells to control microbes in infected tissues, a function in which local random dispersal of a single cell is more important than correlated migration with neighboring cells.

In contrast, CE cells form continuous structures, the capillary blood vessels, by cohort migration, and the earliest step observed during angiogenesis in vitro is in fact a two-cell loop that exhibits a YY pattern [Folkman and Haudenschild, 1980]. Thus, the motility persistence of different cell types might be specifically tuned such that coordinated migration is intrinsically robust in those cell types that have to form congruent structures during morphogenesis. These results also may have implications for tissue engineering because they suggest that functional self-organization of groups of cells in vitro can be achieved by engineering spatially constrained cell populations (e.g., using microfabrication approaches as we did here) with appropriate migratory behavior.

ACKNOWLEDGMENTS

We thank Dr. Robert Mannix for assistance with videomicroscopy, and the laboratory of G. Whitesides and the MRSEC at Harvard University for assistance with the microfabrication.

REFERENCES

Beekman M, Sumpter DJ, Ratnieks FL. 2001. Phase transition between disordered and ordered foraging in Pharaoh's ants. Proc Natl Acad Sci USA 98:9703–9706.

Beloussov LV. 1993. Generation of Morphological patterns: The mechanical ways to create regular structures in embryonic development. In: Stein WD, Varela FJ, editors. Santa Fe Institute Studies in the Sciences of Complexity. Thinking about biology. Reading, MA: Addison-Wesley. p 149–168.

Ben-Jacob E, Cohen I, Gutnick DL. 1998. Cooperative organization of bacterial colonies: from genotype to morphotype. Annu Rev Microbiol 52:779–806.

Brangwynne C, Huang S, Parker KK, Ingber DE, Ostuni E. 2000. Symmetry breaking in cultured mammalian cells. In Vitro Cell Dev Biol Anim 36:563–565.

Brock A, Chang E, Ho CC, LeDuc P, Jiang X, Whitesides GM, Ingber DE. 2003. Geometric determinants of directional cell motility revealed using microcontact printing. Langmuir 19:1611–1617.

Chen CS, Mrksich M, Huang S, Whitesides GM, Ingber DE. 1997. Geometric control of cell life and death. Science 276:1425–1428.

Chen CS, Ostuni E, Whitesides GM, Ingber DE. 2000. Using self-assembled monolayers to pattern ECM proteins and cells on substrates. Methods Mol Biol 139:209–219.

Clark P, Connolly P, Curtis AS, Dow JA, Wilkinson CD. 1991. Cell guidance by ultrafine topography in vitro. J Cell Sci 99:73–77.

Curtis AS, Wilkinson CD. 1998. Reactions of cells to topography. J Biomater Sci Polym Ed 9:1313–1329.

Dike LE, Chen CS, Mrksich M, Tien J, Whitesides GM, Ingber DE. 1999. Geometric control of switching between growth, apoptosis, and differentiation during angiogenesis using micropatterned substrates. In Vitro Cell Dev Biol Anim 35:441–448.

Dunn GA. 1983. Characterising a kinesis response: time averaged measures of cell speed and directional persistence. Agents Actions Suppl 12:14–33.

Dunn GA, Brown AF. 1987. A unified approach to analysing cell motility. J Cell Sci Suppl 8:81–102.

Ermentrout GB, Edelstein-Keshet L. 1993. Cellular automata approaches to biological modeling. J Theor Biol 160:97–133.

Farrell BE, Daniele RP, Lauffenburger DA. 1990. Quantitative relationships between single-cell and cell-population model parameters for chemosensory migration responses of alveolar macrophages to C5a. Cell Motil Cytoskeleton 16:279–293.

Folkman J, Haudenschild C. 1980. Angiogenesis in vitro. Nature 288:551–556.

Gail MH, Boone CW. 1970. The locomotion of mouse fibroblasts in tissue culture. Biophys J 10:980–993.

Glazier JA, Graner F. 1993. Simulation of the differential adhesion driven rearrangement of biological cells. Phys Rev E 47:2128–2154.

Gumbiner BM. 1996. Cell adhesion: the molecular basis of tissue architecture and morphogenesis. Cell 84:345–357.

Haga H, Irahara C, Kobayashi R, Nakagaki T, Kawabata K. 2004. Collective movement of epithelial cells on a collagen gel substrate. Biophys J 88:2250–2256. Epub 2004 Dec 13

Huang S, Ingber DE. 1999. The structural and mechanical complexity of cell-growth control. Nat Cell Biol 1:E131–138.

Kirschner M, Gerhart J, Mitchison T. 2000. Molecular "vitalism." Cell 100:79–88.

Levine H, Rappel W-J, Cohen I. 2001. Self-organization in systems of self-propelled particles. Phys Rev E 63:017101 (4 pages).

Matsuda T, Sugawara T. 1996. Control of cell adhesion, migration, and orientation on photochemically microprocessed surfaces. J Biomed Mater Res 32:165–173.

Moore KA, Huang S, Kong Y, Sunday ME, Ingber DE. 2002. Control of embryonic lung branching morphogenesis by the Rho activator, cytotoxic necrotizing factor 1. J Surg Res 104:95–100.

Murray JD. 1993. Mathematical biology. Berlin: Springer-Verlag.

Nabeshima K, Inoue T, Shimao Y, Kataoka H, Koono M. 1999. Cohort migration of carcinoma cells: differentiated colorectal carcinoma cells move as coherent cell clusters or sheets. Histol Histopathol 14:1183–1197.

Nijhout HF. 1997. Pattern formation in biological systems. In: Nijhout HF, Nadel L, Stein D, editors.Pattern formation in the physical and biological sciences. Lecture Notes Vol. V. Reading, MA: Addision-Wesley. p 269–298.

Palsson E, Cox EC. 1996. Origin and evolution of circular waves and spirals in Dictyostelium discoideum territories. Proc Natl Acad Sci USA 93:1151–1155.

Parker KK, Brock AL, Brangwynne C, Mannix RJ, Wang N, Ostuni E, Geisse NA, Adams JC, Whitesides GM, Ingber DE. 2002. Directional control of lamellipodia extension by constraining cell shape and orienting cell tractional forces. Faseb J 16:1195–1204.

Rappel W-J, Nicol A, Sarkissian A, Levine H, Loomis WF. 1999. Self-organized vortex state in two-dimensional dictyostelium dynamics. Phys Rev Lett 83:1247–1250.

Rietdorf J, Siegert F, Weijer CJ. 1996. Analysis of optical density wave propagation and cell movement during mound formation in *Dictyostelium discoideum*. Dev Biol 177:427–438.

Schock F, Perrimon N. 2002. Molecular mechanisms of epithelial morphogenesis. Annu Rev Cell Dev Biol 18:463–493.

Sells MA, Boyd JT, Chernoff J. 1999. p21-activated kinase 1 (Pak1) regulates cell motility in mammalian fibroblasts. J Cell Biol 145:837–849.

Stocker S. 1999. Models for tuna school formation. Math Biosci 156:167–190.

Stokes CL, Lauffenburger DA, Williams SK. 1991. Migration of individual microvessel endothelial cells: stochastic model and parameter measurement. J Cell Sci 99:419–430.

Turing AM. 1952. The chemical basis of morphogenesis. Phil Trans R Soc Lond B237:37–72.

Uhlenbeck GE, Ornstein LS. 1930. On the theory of Brownian motion. Phys Rev 36:823–841.

van Oudenaarden A, Theriot JA. 1999. Cooperative symmetry-breaking by actin polymerization in a model for cell motility. Nat Cell Biol 1:493–499.

Verkhovsky AB, Svitkina TM, Borisy GG. 1999. Self-polarization and directional motility of cytoplasm. Curr Biol 9:11–20.

Vicsek T, Czirók A, Ben-Jacob E, Cohen I, Shochet O. 1995. Novel type of phase transition in a system of self-driven particles. Phys Rev Lett 75:1226–1229.

Ware MF, Wells A, Lauffenburger DA. 1998. Epidermal growth factor alters fibroblast migration speed and directional persistence reciprocally and in a matrix-dependent manner. J Cell Sci 111:2423–2432.

Zigmond SH, Klausner RD, Tranquillo R, Lauffenburger DA. 1985. Analysis of the requirements for time-averaging of the receptor occupancy for gradient detection by polymorphonuclear leukocytes. In: Czech MO, Kahn CR, editors. Membrane receptor and cellular regulation. New York: Alan R. Liss. p. 347–356.